NOBLE GAS INCORPORATION IN PRESOLAR NANODIAMOND ANALOGS AND RELATED CARBONACEOUS PHASES. R. M. Stroud[1], T. R. Kim [1,2], M. J. Crane[3], and P. J. Pauzauskie[4,5], Naval Research Laboratory, Code 6366, 4555 Overlook Ave. SW, Washington, DC 20375. [2]NRC/NRL Postdoctoral Fellow [3]Dept. Chemical Engineering, University of Washington, Seattle, WA 98195. [4]Dept. of Materials Science and Engineering, University of Washington, Seattle, WA 98195. [5]Physical and Computational Science Directorate, Pacific Northwest National Laboratory, Richland, WA 99352.

Introduction: Meteoritic nanodiamond residues are the carriers of nucleosynthetic isotopic anomalies, including Xe-HL and other noble gas components, which indicate some portion of the residues formed from supernova nucleosynthesis products [1]. However, the overall abundance of these supernova-generated species is low in the residues (<1 Xe per 10^5 nanodiamonds), and the bulk C and N isotope compositions of the residues are within solar system values. Thus, it is difficult to say which individual nanodiamonds are products of supernova processes, rather than solar system or interstellar medium processes.

A variety of formation scenarios for the meteoritic nanodiamonds have been proposed [2], including gentle vapor phase condensation in core-collapse supernovae, shock wave formation in supernovae or the interstellar medium, or by condensation, irradiation or collisional processing within the solar system. To distinguish among the scenarios, comparison of the microstructures, and the noble gas release properties of the nanodiamond residues, with the those of laboratory analogs produced under controlled conditions, has been a useful approach [3, 4]. However, incorporation of noble gases in these samples has required post synthesis ion irradiation, which can introduce lattice defects that may alter the nanodiamond atomic structure and alter the gas release profiles. We have recently developed a method for synthesis of noble-gas bearing nanodiamonds without ion irradiation, through high pressure-high temperature (HPHT) transformation of carbon aerogels in a diamond anvil cell [5]. We present here the results of scanning transmission electron microscopy of these presolar nanodiamond analogs.

Methods: Carbon aerogels were synthesized at the University of Washington from resorcinol, acetonitrile, formaldehyde precursors and a hydrochloric acid catalyst. The mixture was ultrasonicated and allowed to gel for ~ 24 hours. The acetonitrile solvent was exchanged by washing with ethanol 4 times over 5 days. Aerogels were dried under supercritical CO_2 to maintain the pore structure. Finally, the gels were pyrolyzed under N_2 at 900°C for 4 hours to remove oxygen species.

The amorphous carbon aerogels were transformed to nanodiamond under HPHT conditions in a diamond anvil cell (DAC) at the University of Washington. The aerogel was lightly ground to a powder and loaded into the DAC. Liquid Ar was added to infiltrate the aerogel pores, and evenly distribute the applied pressure. The pressure was gradually raised to 16.3 GPa, and heat was applied locally with a Nd-YAG laser. The phase transformation of the aerogel was monitored in situ with Raman spectroscopy to identify the emergence of the diamond phase.

Fragments of the DAC transformation products were analyzed with the Nion UltraSTEM scanning transmission electron microscope at the Naval Research Lab. The UltraSTEM was operated at 60 kV, with a nominal probe size 140 pm and a probe current of 50 -150 pA. Electron energy loss (EEL) spectra were recorded with the attached Enfinium ER spectrometer, and energy dispersive X-ray spectroscopy (EDS) was performed with the Bruker 0.7 sr windowless SDD spectrometer. Additional bright-field TEM images and selected area diffraction patterns were obtained with the JEOL 2200FS operated at 200 kV.

Results: The predominant phase in the transformed material is nanodiamond, with particle sizes varying from regions that are uniformly ~ 3 nm, to other regions with particles as large as 50 nm (Fig. 1). Minor amounts of graphite, and other sp^2 carbon were also found. The incorporation of Ar into the nanodiamond is verified by the EEL spectra showing the Ar edge at 245 eV, spatially associated with the C, exhibiting the characteristic EEL spectrum of nanodiamond (Fig 2). That the feature identified as Ar in the EEL spectra is indeed Ar is confirmed with EDS measurements of the same areas (Fig. 3). A few particles with sp^2 bonded carbon also showed incorporation of Ar.

Discussion: Our results clearly demonstrate that amorphous, nanoparticulate carbons can be transformed under HPHT conditions into noble-gas bearing nanodiamonds that are good analogs for meteoritic nanodiamonds. Furthermore, our laser-heated DAC method can be easily modified to allow for incorporation of wide a variety of volatile (N gas, Ar, Kr, Xe) and non-volatile, (N solids, Si, Te) impurities through selection of the noble gas pressure medium and modification of the carbon

aerogel precursor materials. Although this experiment was not designed to directly mimic any specific cosmic nanodiamond formation scenarios, it is notable that the aerogel precursor materials used include molecular species that are common in astrophysical ices, e.g., simple aromatics, and formaldehyde. Thus, shock processing of organic ices with intermixed with condensed noble gases, either on grains in the outer solar nebula or the proto-solar cold molecular cloud, is a possible natural corollary of this laboratory process.

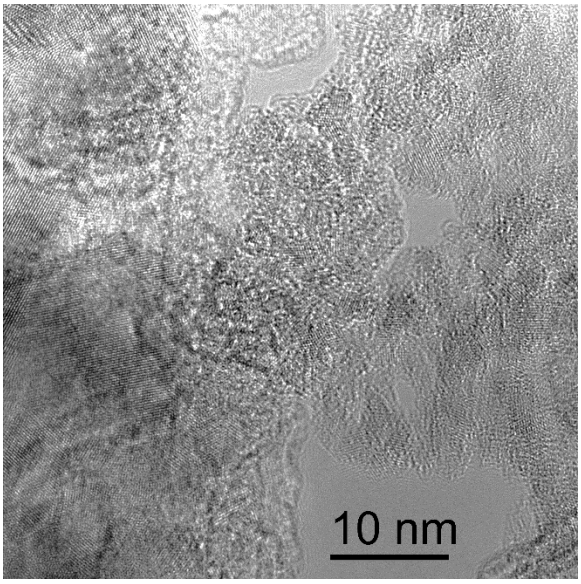

Fig. 1. High-resolution TEM of the HPHT nanodiamonds. Visible lattice fringes correspond to the (111) and (220) spacings of diamond.

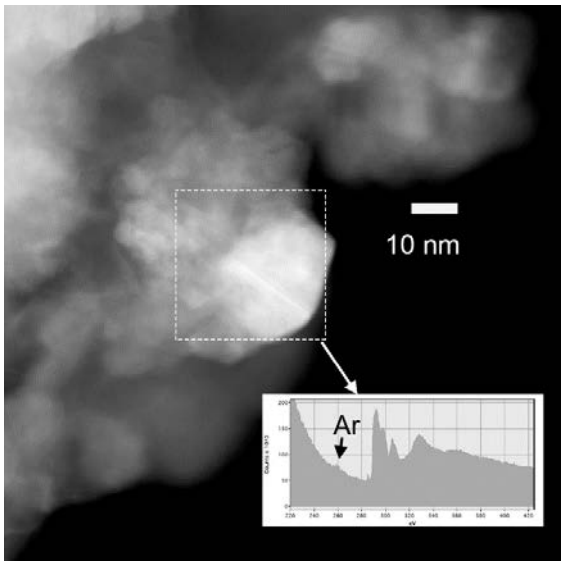

Fig. 2. MAADF STEM image of HPHT nanodiamond. The inset EEL spectrum is the sum spectrum from the area enclosed in the dashed box. The C K edge fine structure is charactertistic of nanodiadmond, and a small Ar adsorption edge is also present.

References: [1] Lewis R. et al. (1987) *Nature, 326*, 160. [2] Ott U. et al. (2012) *Pub. Astron. Assoc. Australi., 29*, 90. [3] Daulton T. et al. (1996) *GCA 60*, 683. [4] Huss G. R. et al (2008) *MAPS, 43*, 1811. [5] Pauzauskie P. J. et al. (2011) *PNAS, 108*, 0550.

Additional Information: RMS acknowledges support for this work from the NASA Emerging Worlds and SSERVI programs. PJP acknowledges support from NSF (CAREER Award #1555007). MJC acknowledges support from from the Department of Defense through a National Defense Science and Engineering Graduate (NDSEG) program.

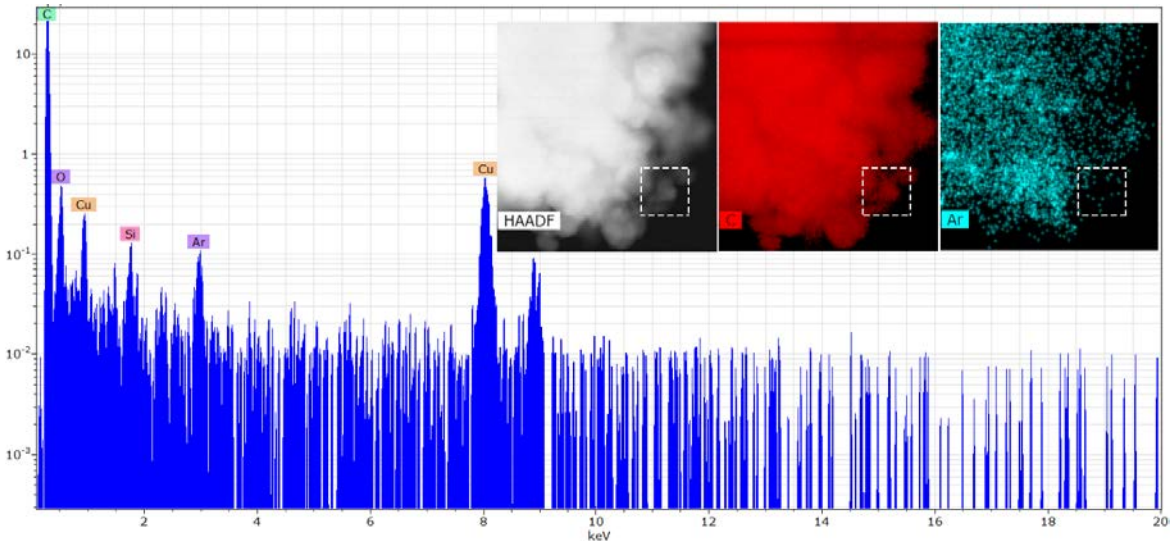

Fig. 3. STEM-EDS elemental maps and extracted sum spectrum. The sum spectra was obtained from the area inside the dashed white box, which corresponds to the field-of-view of Fig. 2.